A novel engineered fusion protein effectively targets and expands disease specific anti-tumor T-cells

Jonathan-Andrew N. Soriano, Joey Lee, Melissa M. Kemp, Dharma R. Thapa, Zohra Merazga, Kelly Malone, Maria Hackett, Luke Witt, Jessica Ryabin, Aaron Zannini, Paige L. Ruthardt, Alyssa Nelson, Lauren D. Kraemer, Emily Christie, Xiang Pan, Ahmet S. Vakkasoglu, Samantha Povlich, Natasha Girgis, Saso Cemerski, Mark Haydock, Emily Spaulding, Steven N. Quayle, Mary C. Simcox, Simon Low, Rodolfo J. Chaparro, Anish Suri, John F. Ross, Ronald D. Seidel, III

Cue Biopharma, Cambridge, MA

Summary

- Cue Biopharma's Immuno-STAT™ (Selective Targeting and Alteration of T Cells) platform is designed to directly engage with and modulate the activity of antigen-specific targeted T cells *in vivo* through a singular molecular framework.
- To develop CUE-100 series biologics, core components were engineered to target via a peptide-HLA complex (pHLA), directing the co-stimulatory molecule (MOD) activity to disease-associated T-cells.
- The affinity of Interleukin 2 (IL-2) for its receptors was modified to reduce interaction with non-target cells while maintaining stimulatory activity (MOD attenuation).
- Manufacturability was confirmed by determination of production and yield following expression in a CHO cell system and purification to homogeneity.
- To demonstrate the utility of the platform, CUE-101, comprised of an effector attenuated human immunoglobulin G (IgG1) Fc domain, an affinity attenuated form of the cytokine IL-2, and a pHLA with a peptide epitope derived from the human papilloma virus E7 protein (HPV16-E7) was generated. CUE-101 demonstrates specific binding to antigen-specific T cells. A murine surrogate has shown antitumor activity in mouse tumor models.

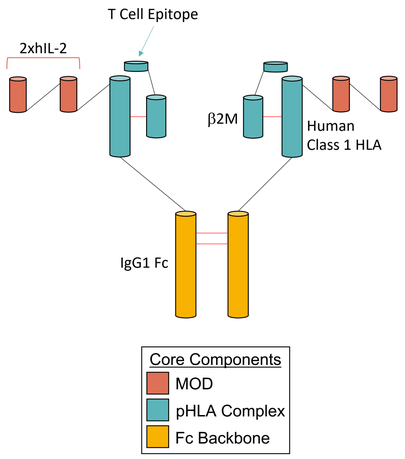

Figure 1 – Diagram illustrating CUE-100 Immuno-STAT (IST) series framework and core components

pHLA Allele and MOD Diversity

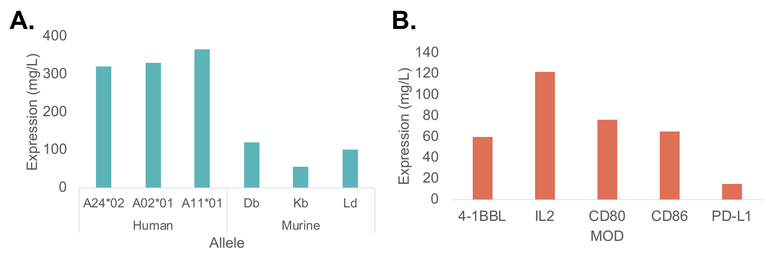

Figure 2 – The CUE-100 framework allows for combinatorial design of unique molecules with stimulatory and inhibitory MODs expressed on a variety of human and mouse MHC alleles. (**A**) Expression titer as measured by Bio-Layer Interferometry (BLI) following transient CHO cell expression indicates high manufacturability of Immuno-STATs containing various human and mouse MHC alleles. (**B**) Expression titer as measured by BLI following transient CHO cell transfection indicates both stimulatory and inhibitory MODs can be successfully integrated onto the CUE-100 IST series framework. PD-L1 was expressed on IST bearing the murine Kd allele and additional MODs were expressed on ISTs bearing the human A02*01 allele.

Peptide Diversity

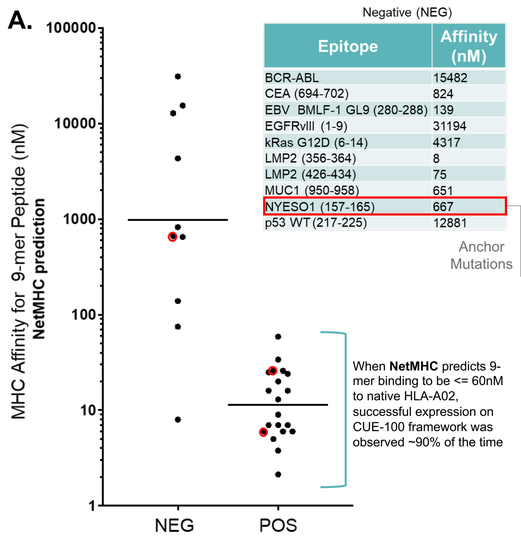

Negative (NEG)

Epitope	Affinity (nM)
BCR-ABL	15482
CEA (694-702)	824
EBV BMLF-1 GL9 (280-288)	139
EGFRvIII (1-9)	31194
kRas G12D (6-14)	4317
LMP2 (356-364)	8
LMP2 (426-434)	75
MUC1 (950-958)	651
NYESO1 (157-165)	667
p53 WT (217-225)	12881

Positive (POS)

Epitope	Affinity (nM)
AFP(126-134)	3
BALF4 (276-284)	4
CEA (571-579)	13
CMV pp65 (495-503)	26
FLU-M1 (58-66)	16
gp100 (154-162)	20
gp100 (209-217)	6
HBVCore (18-27)	34
Her2/neu (369-377;V2V9)	9
KLK4 (11-19)	6
LMP1(125-133)	2
MAGE-A3(112-120)	16
NYESO1 (157-165, C165A)	26
NYESO1 (157-165, C165V)	6
p53 WT (264-272)	24
PAP-3 (135-143)	5
PSMA (4-12)	59
PSMA (27-38)	7
Survivin (96-104)	25
Tyrosinase (369-377, 371D)	7
WT1 (126-134)	7

Anchor Mutations

When **NetMHC** predicts 9-mer binding to be <= 60nM to native HLA-A02, successful expression on CUE-100 framework was observed ~90% of the time

B.

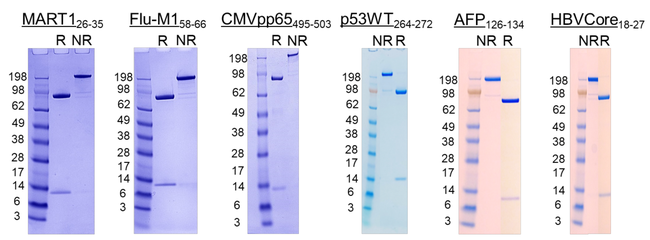

Figure 3 – CUE-100 IST series framework allows for diverse, predictable pHLA expression. (**A**) Peptide sequences from indicated 9-mer epitopes were analyzed by the NetMHC affinity prediction software and grouped into either negative (NEG) or positive (POS) bins depending on initial expression success. A direct correlation was observed between peptide affinity and protein producibility. As demonstrated with NYESO1(157-165) indicated in red, anchor modifications, such as C165A or C165V on NYESO1(157-165), can rescue poor protein production. (**B**) Reduced (R) and non-reduced (NR) SDS-PAGE of representative examples of ISTs bearing 9-mer and 10-mer pHLAs.

Affinity Attenuation of MOD

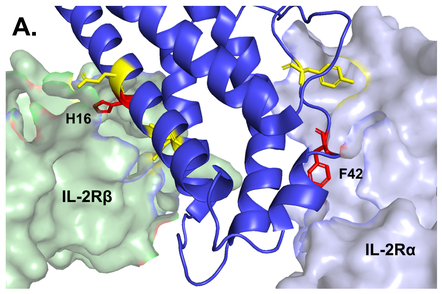

B.

IST+	Exp. (mg/L)
hIL2(wt)	94
hIL2(F42A)	352
hIL2(H16A,F42A)	135
hIL2(D20K,F42A)	311
hIL2(D20L,F42A)	11
hIL2(F42A,N88R)	310
hIL2(D20K,F42A,Q126A)	158
hIL2(D20L,F42A,Q126A)	8
hIL2(F42A,N88R,Q126A)	212
hIL2(E15A,D20K,F42A)	82
hIL2(E15A,D20L,F42A,)	4
hIL2(E15A,F42A,N88R)	204

*Deborah J. Stauber et al. PNAS 2006;103:8:2788-2793

C.

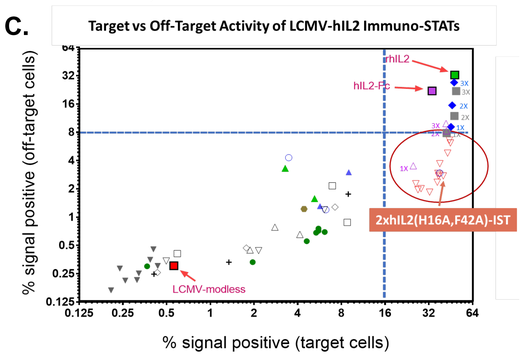

Figure 4 – Protein expression level and biological activity of affinity attenuated hIL-2 both drive MOD selection. (**A**) Diagram depicting IL-2 and its interaction with IL-2R α and β subunits derived from Stauber et. al.* Residues selected for mutation are indicated in yellow and red, with final selected substitutions of H16 and F42 indicated in red. (**B**) Immuno-STATs (ISTs) bearing mutations leading to affinity attenuation of hIL-2 were evaluated for expression following transient CHO cell transfection by BLI. (**C**) Attenuated hIL-2 bearing ISTs were evaluated for biological activity using pSTAT5 staining on target (from LCMV transgenic mice) and off-target (from BL6 mice) CD8⁺ T cells as a measure of target cell specific IL-2 induced signaling. The percentage of pSTAT5 positive cells in both groups was assessed for each IL-2 variant relative to wildtype recombinant IL-2 (rhIL2) in order to select the IL-2 component for the CUE-100 series. 2xhIL2(H16A,F42A) was selected for further characterization.

MOD Cellular Validation

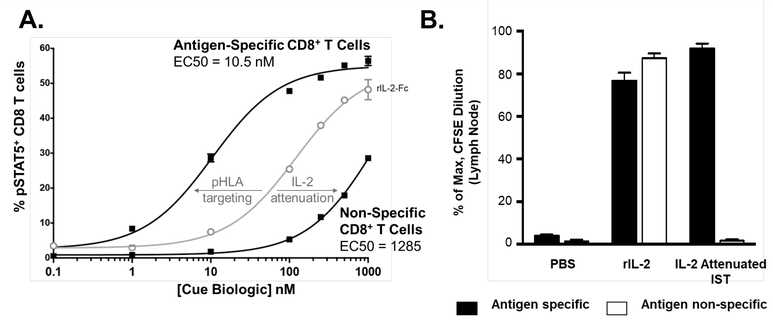

C. Demonstration of signaling attenuation in non-antigen specific T cells

Description	EC_{50}-LCMV	EC_{50}-BL6	Fold Difference (BL6/LCMV)	Δ_{log} EC50
IL-2 Wild Type	42.92	88.53	2.07	0.03
IL-2 Wild Type-Fc	120.8	119.5	0.99	0
IL-2 Wild Type IST	2.89	103.2	35.66	1.55
IL-2 Attenuated IST	10.5	1285	122.38	2.09

D. Demonstration of attenuation to IL-2Rα/β in direct binding studies

		K_D (nM)	$K_{on}(M^{-1}s^{-1})$	$K_{off}(s^{-1})$
wt IL-2	IL-2Rα	10.7 ± 1.4	$5.5x10^5$ ± $1.6x10^5$	$5.8x10^{-3}$ ± $1.5x10^{-3}$
atnu IL-2		1180 ± 124.9	$3.1x10^5$ ± $2.3x10^5$	$5.2x10^{-1}$ ± $0.4x10^{-1}$
wt IL-2	IL-2Rβ	197 ± 1.6	$5.9x10^5$ ± $1.2x10^5$	$1.2x10^{-1}$ ± $0.2x10^{-1}$
atnu IL-2		613.2 ± 31.0	$7.1x10^5$ ± $2.0x10^5$	$4.4x10^{-1}$ ± $1.3x10^{-1}$

Figure 5 – Characterization of attenuated MOD. (**A**) Cue Immuno-STAT, CUE-100-LCMV, bearing the LCMV derived peptide gp_{33-41} in the context of H-2D^b fused to IL-2(F42A,H16A) was used to stimulate antigen-specific splenic CD8⁺ T cells (P14 TCR Tg, C57BL/6 background) versus wildtype C57BL/6 splenic CD8⁺ T cells, and phosphorylation of STAT5 (pSTAT5) measured as a readout of IL-2R signaling. Potency of IL-2R activation on antigen-specific CD8⁺ T cells was enhanced relative to rIL-2-Fc while activation of IL-2R in non antigen-specific CD8⁺ T cells was significantly reduced relative to rIL-2-Fc. rIL-2-Fc did not differentiate between antigen-specific and non-specific cells. (**B**) Splenic CD8⁺ T cells from P14 T cell receptor transgenic mice (CD45.1⁺) and CD8⁺ T cells from wildtype C57BL/6 mice (CD45.2⁺) were labeled with carboxyfluorescein succinimidyl ester (CFSE) and cotransferred into C57BL/6 recipient mice. CUE-100-LCMV or wildtype IL-2 were then administered to recipient mice. Four days later, the degree of T cell proliferation was measured by flow cytometry via CFSE dilution with antigen specific versus non-specific CD8⁺ T cells differentiated by CD45 allelic expression. CUE-100-LCMV selectively enhanced proliferation of antigen specific versus non-specific CD8⁺ T cells *in vivo*, while wildtype IL-2 induced proliferation of both antigen specific and non-specific CD8⁺ T cells equivalently. (n=3-4). (**C**) CD8⁺ T cells from P14 TCR Tg and C57BL/6 mice were isolated from spleens, stimulated with the indicated IL-2 variant, stained with PE-labeled α-pSTAT5, and the resulting fluorescence was quantified to determine % of cells that were pSTAT5 positive. ISTs bearing the attenuated hIL-2 showed a 122.4 fold difference in EC_{50} between antigen-specific and non-specific T cells. (n=4). (**D**) K_D values of wild type (wt) IL-2 and attenuated IL-2 (H16A, F42A) against the cognate receptors were measured directly via BLI. Attenuated IL-2 showed reduced affinity binding to IL-2R α and β subunits.

CUE-100 Manufacturability

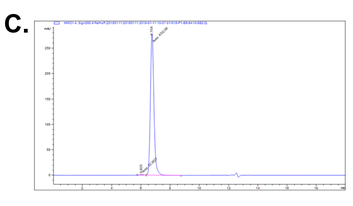

Figure 6 – Resulting optimized CUE-100 IST series framework bearing attenuated MOD demonstrates robust manufacturability. (**A**) Simplified flow diagram of the purification process of CUE-100 IST series proteins. (**B**) Reduced (R) and non-reduced (NR) SDS-PAGE of purified CUE-100-HPV. (**C**) Analytical HPLC-SEC was performed on purified protein and demonstrated >95% homogeneity.

CUE-101 selectively binds antigen-specific T cells

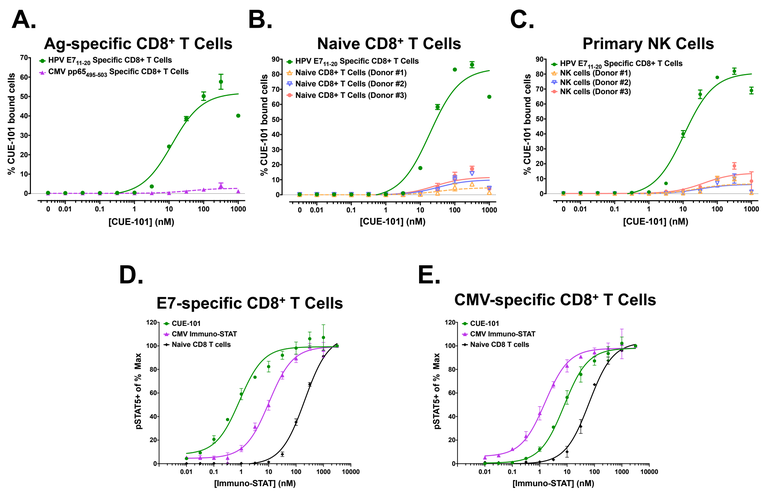

Figure 7 – CUE-101 selectively binds and stimulates signal transduction in human antigen (Ag) - specific CD8⁺ T cells. (**A-C**) CUE-101 potently and selectively binds to E7-specific T cells but not to $CMVpp65_{495-503}$-specific T cells (**A**), primary naïve CD8⁺ T cells (**B**), or primary NK cells (**C**) that also express IL-2 receptor (IL-2R). (**D-E**) The pHLA specificity of CUE-101 enables potent and selective stimulation of phosphorylation of STAT5 (pSTAT5) immediately downstream of IL-2R engagement on target T cells. (**D**) CUE-101 (HPV-directed) induces pSTAT5 with greater potency in $E7_{11-20}$-specific CD8⁺ T cells than does a CMV-directed Immuno-STAT. (**E**) A CMV-directed Immuno-STAT induces pSTAT5 with greater potency in CMV $pp65_{495-503}$-specific CD8⁺ T cells than does CUE-101. Induction of pSTAT5 is further reduced in naïve CD8⁺ T cells relative to activated antigen-specific CD8⁺ T cells.

CUE-101 murine surrogate inhibits tumor growth in the TC-1 syngeneic model

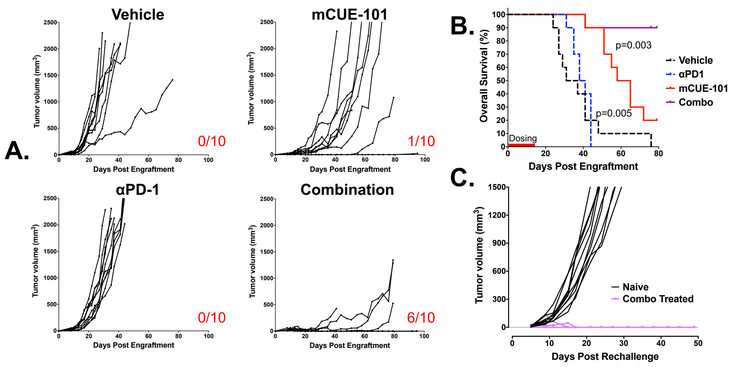

Figure 8 – CUE-101 murine surrogate (mCUE-101) inhibits TC-1 syngeneic tumor growth alone and in combination with αPD-1 blockade, and generates immunologic memory. (**A**) Spider plots of individual tumor volume growth following treatment with the indicated agents. The frequency of tumor-free mice at Day 90 post-injection is indicated. (**B**) Kaplan-Meier survival analysis confirms single agent mCUE-101 significantly extends overall survival in this model, with significant further survival upon combination treatment with αPD-1. (**C**) Mice remaining tumor-free after combination treatment were re-challenged with TC-1 tumors 97 days post primary tumor challenge. While naïve mice all formed tumors, previously treated animals rejected tumor formation, thus demonstrating functional immunologic memory.

Conclusions

Cue Biopharma's Immuno-STAT platform exploits rational protein engineering to generate therapeutic molecules for selective T cell modulation in immuno-oncology, autoimmunity, and chronic infectious diseases. The core engineered framework is comprised of a MOD, a pHLA complex, and an Fc backbone. The CUE-100 series of biologics allows for incorporation of both stimulatory or inhibitory MODs, which are expressed with human or mouse MHC Class I alleles bound to diverse peptides within a predictable range of binding affinity. MOD selection is driven by both manufacturability and specific biological activity, which can be validated through *in vitro*, *ex vivo*, *in vivo*, and direct ligand-receptor binding assays. The modularity and flexibility of the Immuno-STAT platform allows for incorporation of diverse MHC alleles, antigenic peptides, and relevant biological signals, which can be applied to target different disease indications.

The lead candidate, CUE-101, selectively binds and stimulates TCR and IL-2R-mediated signal transduction in antigen-specific CD8⁺ positive T cells *in vitro*. A murine surrogate, mCUE-101, inhibits TC-1 syngeneic tumor growth alone and in combination with αPD-1 blockade, as well as generates immunologic memory. The novel mechanism of action of CUE-101, namely targeted activation of tumor-antigen-specific CD8⁺ T cells via delivery of reduced affinity mutant IL-2, supports its increased potential for anti-cancer efficacy and reduced toxicity relative to non-targeted forms of immunotherapy.

Presented at the Protein Engineering Summit (PEGS) • April 8-12, 2019 • Boston, MA